Current Biology, Volume *23*

Supplemental Information

Fission Yeast Does Not Age under Favorable Conditions, but Does So after Stress

Miguel Coelho, Aygül Dereli, Anett Haese, Sebastian Kühn, Liliana Malinovska, Morgan E. DeSantis, James Shorter, Simon Alberti, Thilo Gross, and Iva M. Tolić-Nørrelykke

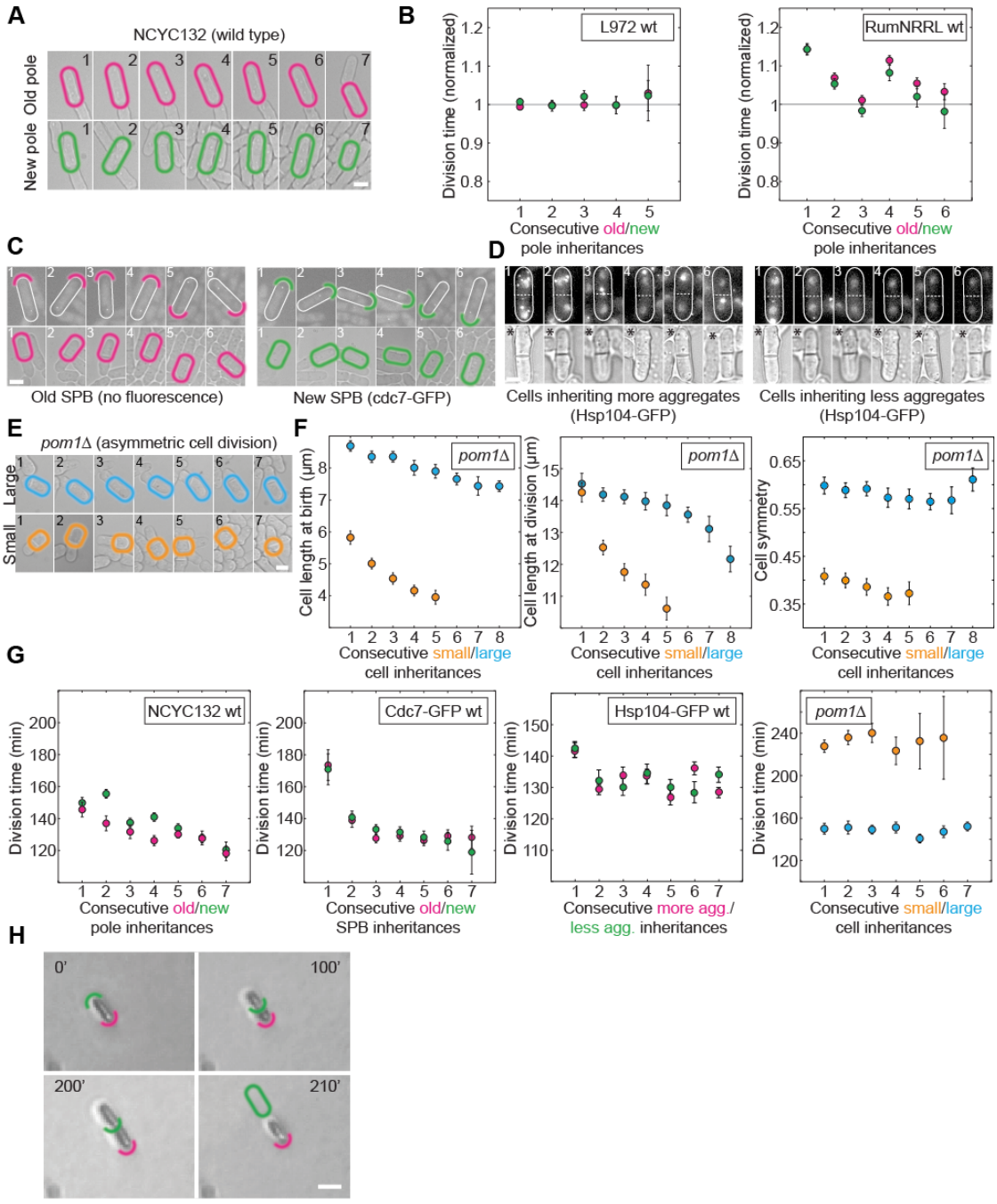

Figure S1. Aging Factors Do Not Correlate with Aging in *S. pombe* for Several Consecutive Divisions, Related to Figure 1

(A) Morphology of cells consecutively inheriting the new (green) or the old (magenta) cell pole is shown for NCYC132 strain. No round shaped cells were observed. (B) L972 and RumNRRL wild type cells that inherited the old or the new pole. L972 old-pole cells showed an average increase in division time by 0.0072 per division, r=0.78, 95%-confidence interval

for r=[-0.34, 0.98], p = 0.12. New-pole cells showed an average increase in division time by 0.0033 per division, r = 0.43, 95%-confidence interval for r = [-0.73, 0.95], p = 0.47 (semi-automated analysis; n=10 cell lineages, n>30 cells). RumNRRL wild type cells that inherited the old or the new pole. Old-pole cells showed an average decrease in division time by 0.0140 per division, r = -0.53, 95%-confidence interval for r = [-0.94, 0.50], p = 0.28. New-pole cells showed an average decrease in division time by 0.0231 per division, r = -0.69, 95%-confidence interval for r = [-0.96, 0.27], p = 0.13 (semi-automated analysis; n=24 cell lineages, n>30 cells). (C) Morphology of cells consecutively inheriting the new (green) or the old (magenta) spindle pole body (cdc7-GFP labels the new SPB), (D) more (magenta) or less (green) protein aggregate amount (Hsp104-GFP labels the new SPB), and (E) pom1 mutant cells consecutively inheriting a larger (blue) or smaller (yellow) cell volume. (F) Cell length at birth and division and symmetry at division of the pom1 mutant strain, for larger (blue) or smaller cells (yellow) is plotted for consecutive divisions (n>30 cells for each division). (G) Non-normalized cell division times for the consecutive inheritance of cellular components (aging factors) described in Figure 1B-E. (H) Cell pole inheritance and micromanipulation of dividing fission yeast cells. We followed cells consecutively inheriting the old or the new pole by using a micromanipulation technique: starting with a spore, individual cells inheriting the old or the new pole were kept on an agar plate while all other cells were removed by using a microneedle to the periphery of the agar plate after each 1-3 cell divisions. Cell poles are marked with magenta (old) and green (new) arcs. Green oval shows the previous position of the discarded cell. Data are mean±SEM, scale bars = 5 μm.

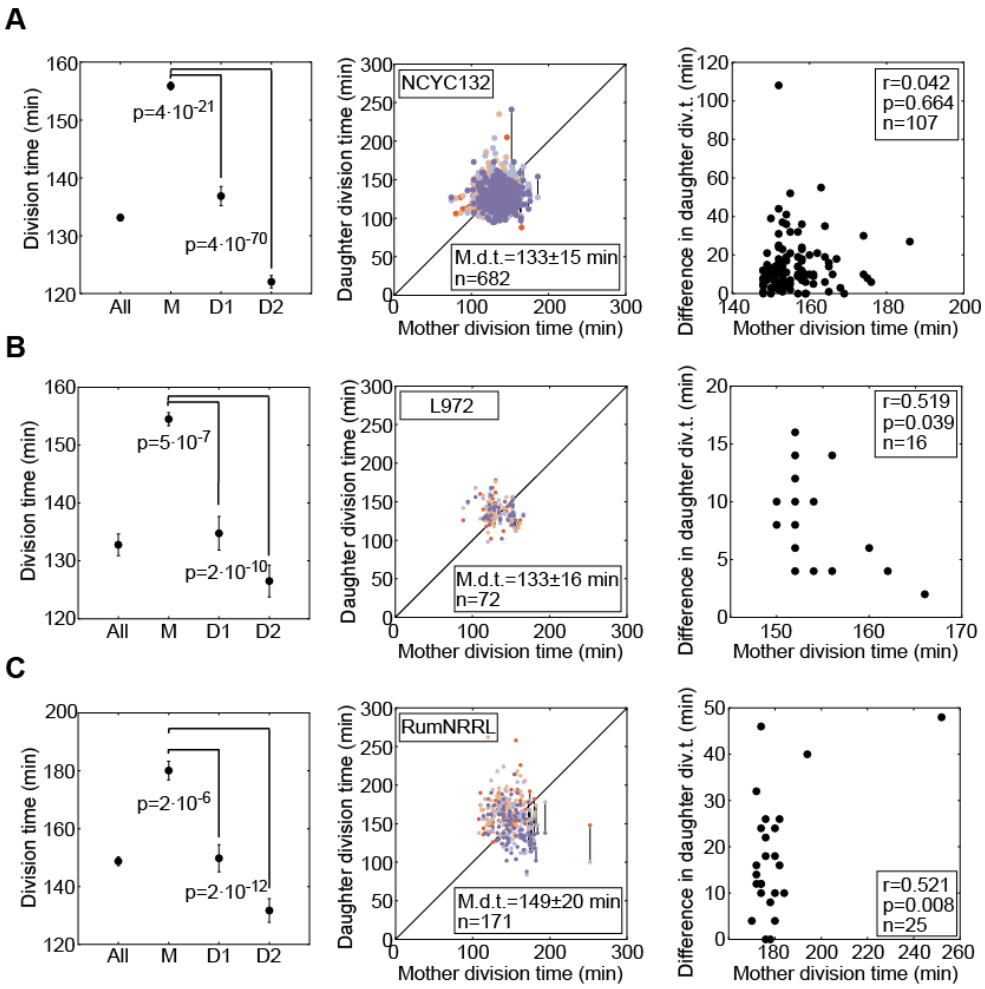

Figure S2. Correlation between the Mother and Daughter Division Times for Different Wild-Type Strains Shows No Increase in Division Time in the Daughters, Related to Figure 2

(A) NCYC132 wild type**,** (B) L972 wild type**,** (C) RumNRRL wild type**.** In the left panels, we compare the average division time of all mothers, "old" mothers (those with the division time 1 s.d. above the average, *M*), "old" daughters (daughter that divided slower than their siblings, *D1*) and "young" daughters (daughters that divided faster than their siblings, *D2*). *P*-values from a t-test comparing mothers and daughters are also shown. In the middle panels, daughter division times are plotted as a function of the mother division times (M.d.t.). In the right panels, the difference in the division time between the two daughter cells is shown as a function of the mother division time. Correlation coefficients *r* and the corresponding *P*-values are reported; *n* = number of cells. For the strain RumNRRL, an outlier cell was removed (mother cell division time 260 min, high above the average for "old mothers" (180min)).

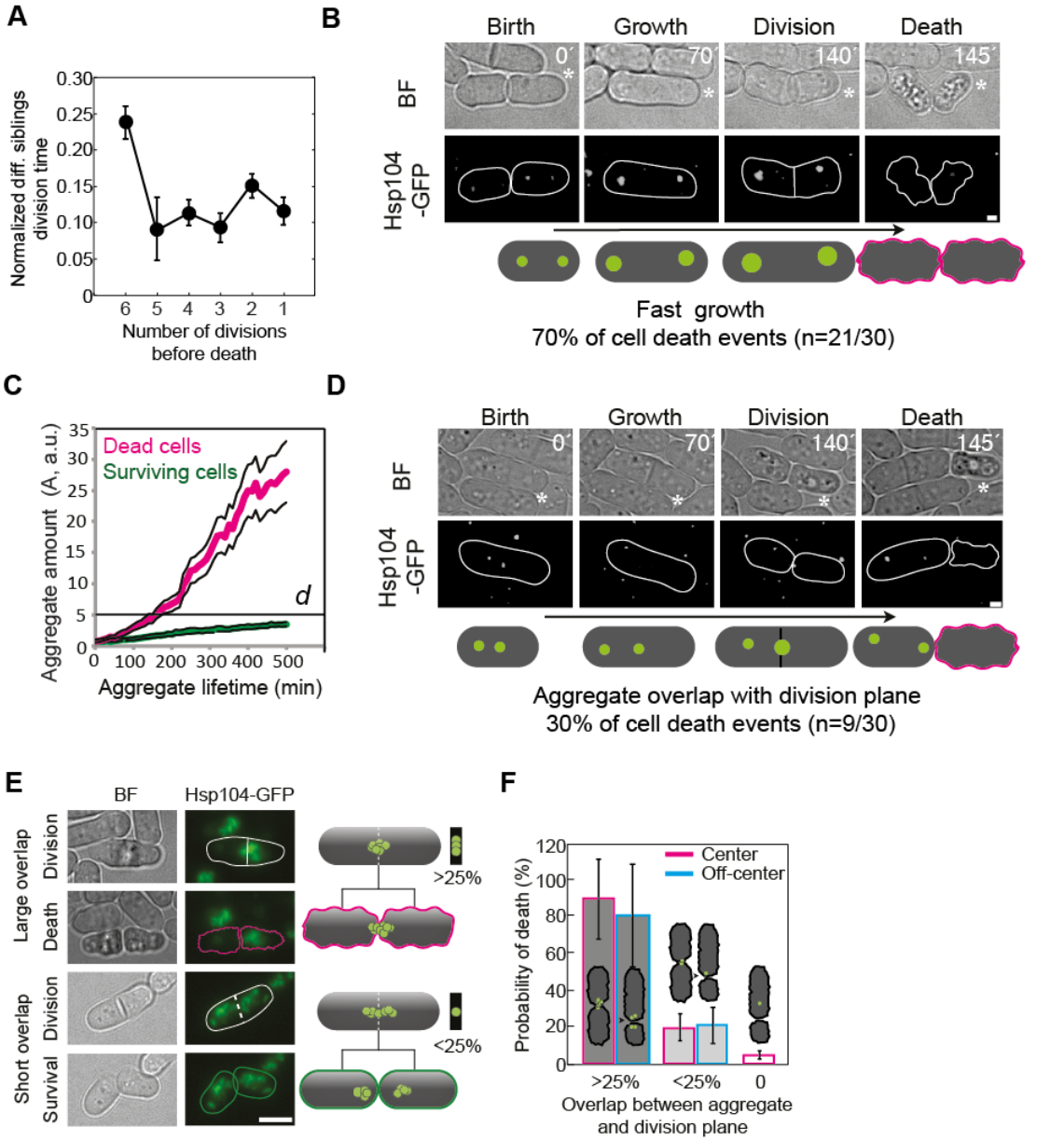

Figure S3. Division Time between Siblings Does Not Increase before Death and Aggregate Growth and Overlap with Division Plane Correlates with Catastrophic Cell Death, Related to Figures 3 and 4

(A) The difference in sibling division time does not increase before death (n=32 cell death lineages). (B) Fast growth of aggregates preceding cell death (70% of death events, see also Figure 4A). (C) Total aggregate amount (Hsp104-GFP intensity, a.u.) for individual aggregates over time in cells that eventually died (green, *n*=16 aggregates) and in cells that did not die (grey, *n*=21 aggregates); thin black lines mark SEM. (D) Aggregates localize in the cell center with the division plane and the cell subsequently dies (30% of death events). A white asterisk marks the cell that will die. (E) Time lapse representing cell division events in

Hsp104-GFP cells (MC19 strain), where the protein aggregates overlap with the division plane. If the extent of the overlap is higher than 25% of the length of the division plane, the cell typically dies. (F) Quantification of cell death when aggregates overlap with the division plane, in cell center and off-center events in pom1Δ Hsp104-GFP cells (MC75 strain) (n events > 30 for each bar). Data are mean±SEM; Thin lines encircle cells; Scale bars = 5 μm.

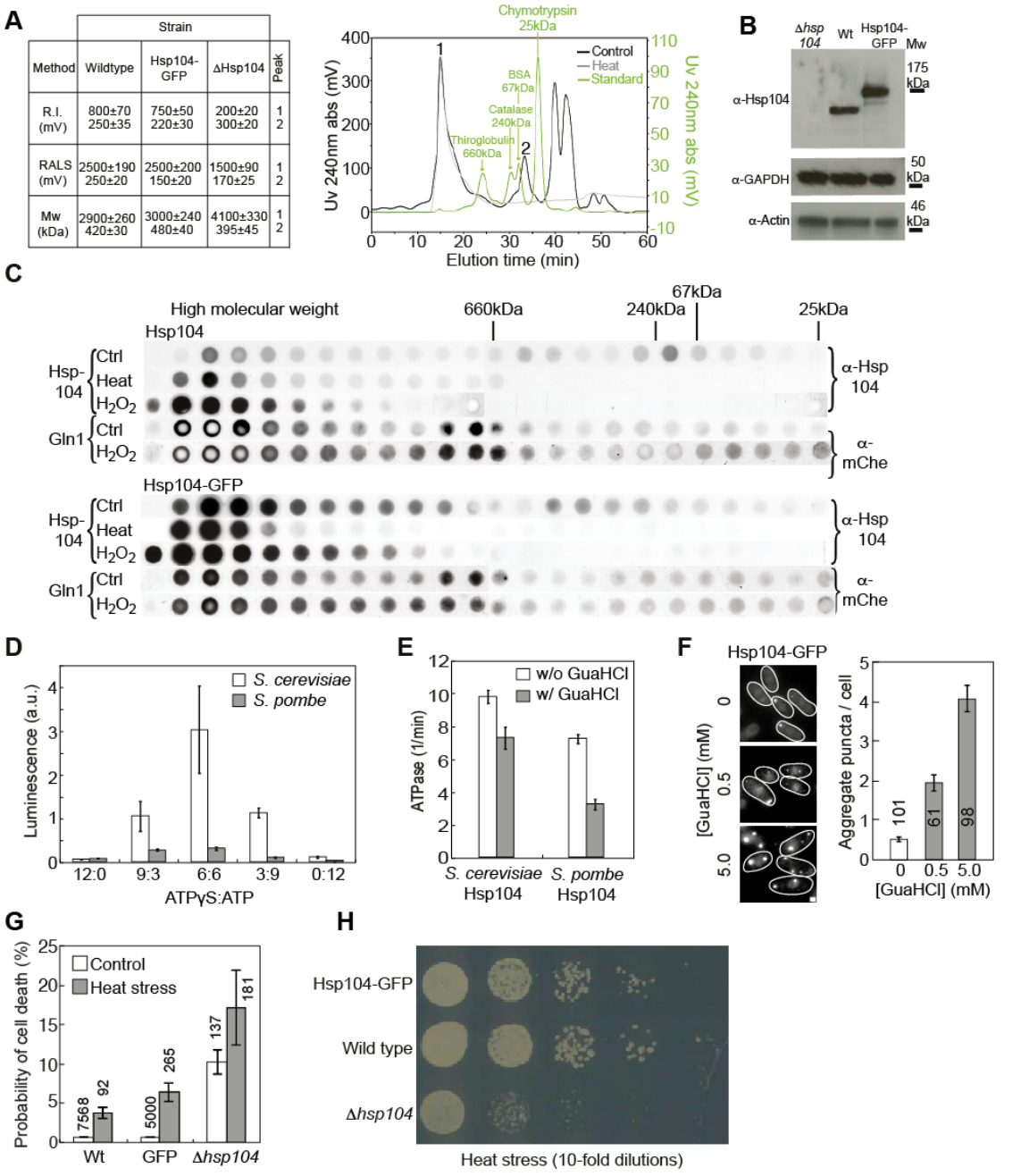

Figure S4. Biochemical Characterization of Protein Aggregates and Hsp104 Function in *S. pombe*, Related to Figure 4

(A) *left*, Table containing the Refractive Index (R.I.), the Right Angle Light Scattering (RALS) and the estimated Molecular weight (Mw) values of high (peak 1) and low (peak 2) molecular weight fractions. Peak 1 corresponds to highly refractive and highly anisotropic light scattering molecules (high RALS value), which most likely are aggregated proteins; *right*, Size exclusion chromatograms (Superose 6 column, molecular weight range 10^4-10^7 Da, $UV_{\lambda=240nm}$ absorption) of wild-type cells in favorable growth conditions and after heat

stress (T=40°C, 1h). (B) Immunodetection of endogenous Hsp104 (wild type, strain L972) and Hsp104-GFP fusion proteins (strain MC19) with the anti-Hsp104 R5 antibody (black indicates protein). GFP was fused to the C-terminus of the Hsp104 gene and is under the control of the native Hsp104 promoter. The signal was absent in a strain deleted for Hsp104 (ΔHsp104, strain MC76). The same antibody was used in Figure S4C. (C) Immunodetection of size exclusion chromatography fractions of Hsp104 (top) and Hsp104-GFP (bottom, black dots are fractions spotted onto nitrocellulose) expressing cells. Note that the Hsp104-GFP fusion (125kDa) eluted above the 240kDa (monomer) and 660kDa (hexamer) standards, respectively, and also in the megadalton range, thus showing similar behavior as native Hsp104. Under oxidative stress, Hsp104-GFP was shifted towards high molecular weight, as observed for endogenous Hsp104. In the presence of Hsp104-GFP fusion, Gln1-mCherry has a similar elution profile as with the endogenous unlabeled Hsp104, indicating that the GFP moiety did not increase aggregation of Gln1. (D) *In vitro* luminescence recovery of urea-denatured luciferase, incubated with either *S. cerevisiae* or *S. pombe* Hsp104 (1μM hexamer) for 90 min at 25°C. Reactions were supplemented with different ratios of ATPγS:ATP as indicated. Total nucleotide concentration was maintained at 5mM; n=4. Note that the relative activity of *S. pombe* Hsp104 was much lower. (E) The graph shows the *in vitro* ATPase activity of 0.25μM *S. cerevisiae* or *S. pombe* Hsp104 at 25°C in the presence or absence of guanidine hydrochloride (GuaHCl) (20mM); n=3-6. (F) *Left*, cells expressing Hsp104-GFP treated with GuaHCl. *Right*, puncta number per cell as a function of GuaHCl concentration. Thin lines indicate cell boundaries; scale bar=1μm. (G) Death frequency of the unlabeled Hsp104 (Wt), Hsp104-GFP (GFP) and Hsp104 deleted (Δ) strains under control conditions and after heat stress (40°C for 1h). (H) Heat stress survival assay of the wild-type L972 strain (Wt), the Hsp104-GFP expressing strain (Hsp104-GFP), and a strain where Hsp104 was absent (ΔHsp104). Serial dilutions of cells were plated after heat stress (40°C for 1h) and grown for two days at 30°C. The wild type and Hsp104-GFP strains show similar growth, while in the absence of Hsp104 the number of surviving cells is reduced. Data are shown as mean±SEM, number of cells are given in the graphs.

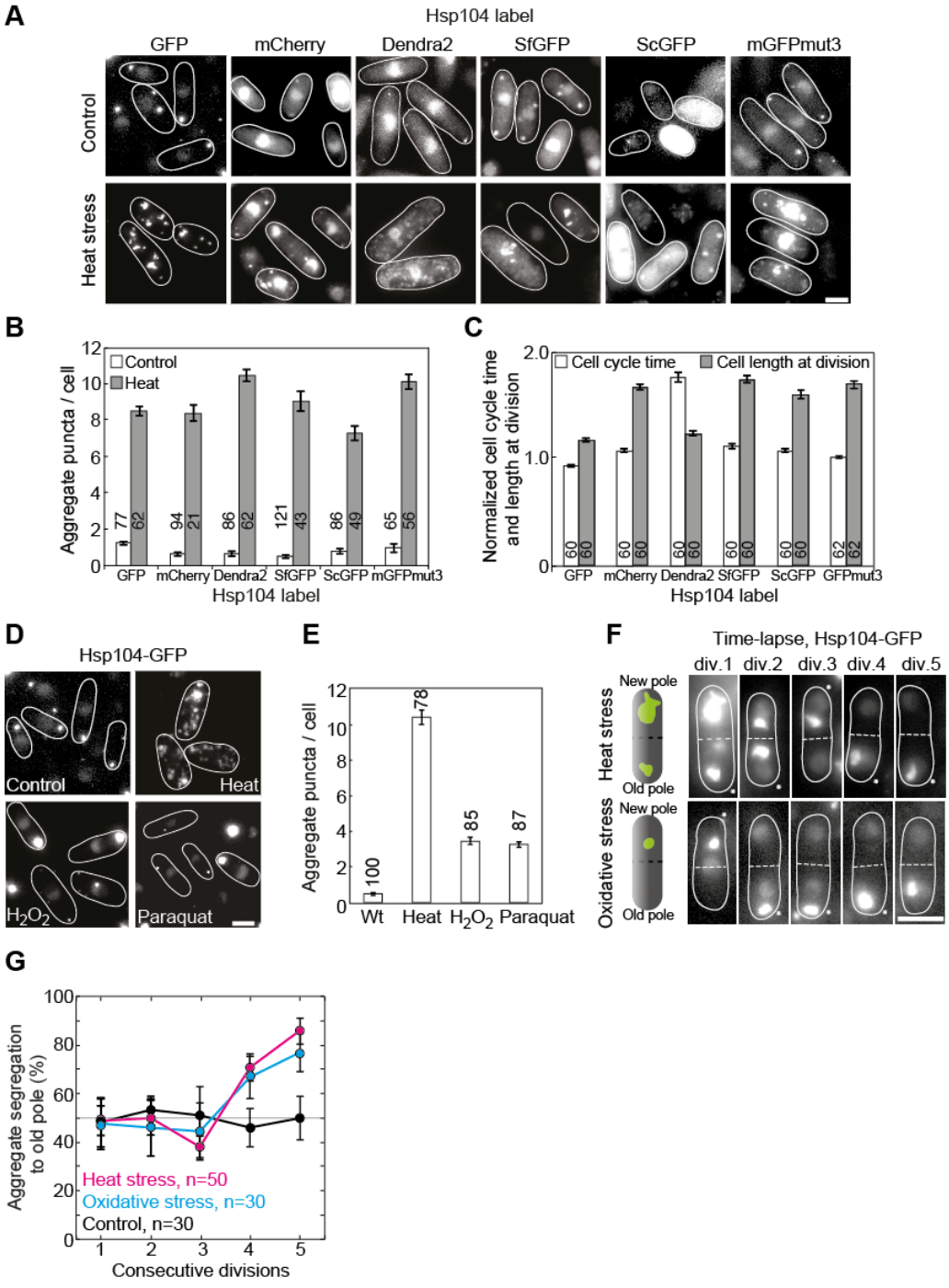

Figure S5. Hsp104 Labeled with GFP Is a Reliable *In Vivo* Marker for Protein Aggregates, Related to Figure 5

(A) Fluorescence images of live cells expressing Hsp104-GFP, Hsp104-mCherry, Hsp104-Dendra2, Hsp104-Superfolder GFP (SfGFP), Hsp104-Super negatively charged GFP (-32, ScGFP), and Hsp104-mGFPmut3. All fusion proteins form cytoplasmic puncta, under control conditions and stress. In addition to cytoplasmic puncta, we also observed a diffuse nuclear

signal, as reported for *S. cerevisiae* (see ref.[S1]). (B) Puncta number per cell under control conditions and after heat stress for the strains shown in A (see labels). (C) Cell cycle duration and cell length at division for the Hsp104-fluorescent protein fusion strains normalized by the wild-type (cell cycle time = 143.2 ± 1.1min, cell length at division = 13 ± 1.6 μm, $n_{cell\ cycles}$=192). As shown before [S2], we observed that cell division was not correlated with cell cycle length. The Hsp104-GFP strain is the most similar to wild type. (D) Live-cell images of Hsp104-GFP cells. Hsp104 localized to cytoplasmic puncta and the nucleus, in control and stress conditions (Paraquat, 1mM for 1h). (E) Average puncta number per cell of cells shown in D. (E) Scheme and time-lapse of Hsp104-GFP cells (MC19 strain) subjected to heat (T=40˚C, 1h) and oxidative (H_2O_2 1mM, 1h) stress. Large aggregates are formed and inherited by one cell at division (old or new pole cell). (F) Time-lapse and (G) quantification of segregation of large aggregates to cells that inherit the old pole over consecutive divisions after stress. In division 4 and 5 there is a bias towards the old cell pole, for both types of stress, but not for the unstressed control. Data are mean±SEM, number of cells are shown in the graphs, scale bars=5μm.

Table S1. Comparison between *S. pombe* Strains and Conditions Used to Study Aging in This and Previous Works, Related to the Discussion

	Strain	Media	T	Total division number	Death	Division time	Changes in morphology
Barker & Walmsley, 1999	NCYC132 h90	2%peptone, 1%yeast extract, 2%glucose, 2%agar	25˚C day, 8˚C o/night	10	15%	-	Cell shape is round
Minois et al, 2005	DSMZ no.70577	YPD	30˚C	-	-	-	Higher carbonylation
Erjavec et al, 2008	L972 h-	YES (1% yeast extract, 3%glucose),	30˚C	13 – old sibs, 16 – young sibs	10%	150min – young cell 270min – old cell	Fission scars; Higher carbonylation
This study	NCYC132 h90, L972 h-, RumNRRL h-, cdc7-GFP h-	YES (1% yeast extract, 3% glucose)	30˚C	No limit up to 50	0,3% (sto-chastic)	140-160 min	None
	*pom1*Δ h-		30˚C	No limit	-	150 (large cell); 300 min (small cell)	None
	MC19 (Hsp104-GFP)		40˚C (1h)	4-5	50%	140-300min; 200 – 900min	None
			30˚C, H_2O_2 1mM	2-3			

Other authors have observed that individual fission yeast cells acquire changes in cell morphology (increased volume, inheritance of fission scars) and have an increased division time. The authors attribute these changes to aging, further demonstrating variation in the carbonylated proteins in the population [S3], similarly to what was found for *S. cerevisiae* [S4]. In another study on *S. pombe*, carbonylated proteins were shown to segregate symmetrically between the two daughter cells [S5], which is consistent with the absence of aging. Aging was also correlated with the accumulation of fission scars [S3, 6], contrary to a theoretical study that predicts a low probability for accumulation of fission scars due to the bipolar growth and symmetrical division character of *S. pombe* [S7].

Table S2. Strains Used in This Study, Related to the Experimental Procedures

Name	Genotype	Source	Growth condition
NCYC132	*Wild-type h90*	Lindner (1893), East African millet beer	30˚C, YE
L972	*Wild-type h-*	Leupold (1970)	30˚C, YE
PYCC4181 (RumNRRL)	*Wild-type h-*	Portuguese yeast culture collection, Rum isolate (1960)	30˚C, YE
IH1106 (cdc7-GFP)	*Cdc7-GFP::ura4+ ura4-D18 h-*	Sohrmann et al (1998)	30˚C, YE
JB110 (*pom1*Δ)	*pom1::ura4+ ura4–D18 h-*	Bahler (1998)	30˚C, YE
MC19	*Wild-type h- hsp104-GFP-kanr*	This study	30˚C or 40˚C, YE or YE 1mM H_2O_2
MC75	*pom1::ura4+ hsp104-GFP-kanr ura4–D18 h-*	This study	30˚C or 40˚C, YE
MC76	*hsp104::kanr ade-M216 ura4-D18 leu1-32 h+*	This study	30˚C or 40˚C, YE
MC92	*hsp104-mCherry-kanr h-*	This study	30˚C or 40˚C, YE
MC157	*hsp104-Dendra2-hphr h-*	This study	30˚C or 40˚C, YE
MC300	*hsp104-SfGFP-kanr h-*	This study	30˚C or 40˚C, YE
MC302	*hsp104-ScGFP-kanr h-*	This study	30˚C or 40˚C, YE
MC310	*hsp104-mGFPmut3-kanr h-*	This study	30˚C or 40˚C, YE

SUPPLEMENTAL EXPERIMENTAL PROCEDURES

1 - Analysis of protein aggregates in *S. pombe* and validation of Hsp104-GFP as a live marker for aggregated proteins. As a first step to investigate protein damage segregation in *S. pombe*, we tested whether *S. pombe* cells contain aggregated proteins. We subjected the lysate of these cells to size exclusion chromatography coupled to dynamic light scattering [S8]. We detected a high molecular weight fraction with a high refractive index that scatter light anisotropically (Figure S4A, peak 1). In *S. cerevisiae*, aggregated proteins have been shown to interact with the chaperone Hsp104 [S9], a disaggregase that recognizes and disassembles aggregated proteins [S10, 11]. We found that the high molecular weight fraction of *S. pombe* lysate contained Hsp104 (Figure S4C). In response to heat and oxidative stress, conditions known to increase protein aggregation [S12, 13], we observed a shift in the distribution of Hsp104 to higher molecular weight fractions, suggesting that aggregates titrated Hsp104 (Figure S4C). We further tested whether glutamine synthetase 1 (Gln1), a metabolic enzyme known to form aggregates in budding yeast [S14, 15], co-eluted with Hsp104 in high molecular weight fractions after oxidative stress (Figure S4C). Indeed, the Hsp104 disaggregase and the gln1 aggregation-prone protein were present in the same high molecular weight fractions. Based on these findings, we conclude that protein aggregates are present in *S. pombe* and associate with Hsp104.

1.1. Hsp104 disaggregase activity reduces aggregate number and size. Based on the observed presence of Hsp104 aggregates in the cell under favorable growth conditions, we wanted to understand to what extent Hsp104 activity controls the number and size of these aggregates. Although the *in vitro* activity of Hsp104 in *S. pombe* was lower than that of *S. cerevisiae*, which may account for the higher number of visible aggregate puncta *in vivo* in *S. pombe*, *S. pombe* Hsp104 was able to disassemble protein aggregates *in vitro* (Figure S4D). The presence of guanidine hydrochloride, a known Hsp104 disaggregase activity inhibitor [S16], resulted in decreased ATPase activity *in vitro* (Figure S4E) and increased the number and size of Hsp104-GFP puncta *in vivo* (Figure S4F). Thus, Hsp104 is an active disaggregase required to reduce aggregate number and size. Also, we noted that cell survival was reduced in a strain lacking Hsp104, both under favourable and stressful growth conditions (Figure S4G and S4H).

1.2. Hsp104-GFP puncta represent physiologically occurring aggregates. By comparing a strain with unlabeled and GFP-labeled Hsp104, we found that the estimated molecular weight of aggregates (Figure S4A, table) and the distribution in different molecular weight fractions was unchanged (Figure S4C). Cell survival under favourable growth conditions or in a thermo-tolerance assay was equally unaffected (Figure S4G and S4H), suggesting that the GFP labeling neither interferes with Hsp104 function nor induces cytotoxicity. Self-oligomerization of GFP can induce the formation of aberrant protein bodies [S17]. To exclude the possibility that Hsp104-GFP puncta in unstressed conditions are a result of GFP self-association, we labeled Hsp104 with fluorescent proteins that do not self-oligomerize [S17]. As can be seen in Figure S5A-C, Hsp104 labeled with non-oligomerizing fluorescent proteins also produced cytoplasmic puncta and a diffuse signal inside the nucleus. The labeling of Hsp104 with mCherry and Dendra2 did not change the occurrence of puncta. Furthermore, labeling of Hsp104 with GFP proteins designed to prevent unfolding and aggregation (Superfolder-GFP), or oligomerization (mut3-GFP and Super-negatively charged GFP(-32)) also resulted in the formation of a similar number of puncta (Figure S5B, see also [S17]) as the original Hsp104-GFP version. This indicates that GFP does not induce oligomerization or aggregation *per se* and that the puncta formed under unstressed or stressed conditions are not an artifact of Hsp104 labeling (Figure S5D). We decided to use the Hsp104-GFP strain: of all the strains where Hsp104 was labeled with a fluorescent protein, it was the one with cell cycle properties most similar to the wild type (Figure S5C). The aggregates formed under unstressed conditions are most likely a result of metabolic stress or errors in translation that occur during cell growth under rich conditions [S18].

2 - Cell death is correlated with accumulation of Hsp104 aggregates. Under favorable growth conditions, a fraction of cells died (0.70±0.14%, n=7568). Cell death was phenotypically identified by the shrinkage of the cell to an irregular shape and darkening of the cytoplasm. Death typically occurred immediately after cell division. After these morphological changes occurred, cell growth stopped, together with the movement of lipid droplets in the cytoplasm. As previously described, these changes in morphology result in the internalization of acridine orange, a dye that marks cellular viability, indicating metabolic death [S19]. Cells that were identified as dead did not exhibit recovery of cell shape nor growth during the remaining divisions of the colony, while surviving cells grew and divided uninterruptedly until the end of the experiment (10h to 20h). Cells in the vicinity of the dead cell did not exhibit death or growth defects, indicating that death was not a localized response

to changes in the growth media. How is cell death linked with aggregate segregation? One possible explanation for the observed "sudden death" after division is that aggregates close to the cell membrane block the access of cytoplasmic cell wall synthesizing enzymes, leading to a weaker cell wall and plasmolysis under the turgor pressure of the cell. This is supported by the correlation between the overlap of aggregates with the division plane and cell death (Figure S3F), which sometimes leads to the death of both siblings.

3 – Materials and methods

Fission yeast culture and genetic manipulation. Cells were grown as described before [S20]. For imaging, cells were transferred to a MatTek dish (MatTek, Ashland, USA) and imaged in liquid media (YE5 or EMM) or covered with a solid agarose pad (YE5-4% Agarose, SeaKem, Hessisch Oldendorf, Germany) at 30°C. Strains were constructed using a PCR based gene targeting technique [S21], where the label was inserted in the C-terminal region of the target gene in the native genomic locus, keeping it under the control of native expression regulators.

Cell preparation for pedigree analysis. Pedigree analysis of a whole microcolony is crucial for studies of aging because it provides data on each individual cell. As the colony grows, it becomes multi-layered and too large for imaging, hence the cells can be followed only through a small number of divisions (6-7). To determine the variation in division time as the number of divisions increases, we observed individual fission yeast cells, randomly selected from an exponentially growing culture, as they repeatedly grew and divided forming a monolayer microcolony under conditions of uninterrupted cell growth, on yeast extract (YE)-4% agarose pads at 30ºC. NCYC132 wild-type cells (originally extracted from east African Millet beer, 1921) were grown in liquid YE media (25ºC). Cells growing in exponential phase (OD=0.1-0.6) were diluted to a final OD of 0.01. This dilution was optimized to ensure that single disperse cells could be observed. A volume of 10µl of cells was transferred to a MatTek (MatTek Corp., Ashland, USA) dish. A thin YE-4% agarose pad was placed on top of the cells. The pad was covered with a coverslip and sealed with vaseline. Then two squares of wet Whatman paper (Biometra, Goettingen, Germany) were placed inside the dish to prevent the pad from drying. The dish was sealed with the lid and wrapped in parafilm. This allows the cells to grow in an oxygenated and nutrient rich hydrated environment during the time course of the experiment. The strains used in this work (NCYC132, L972 h-,

RumNRRL, *pom1*Δ) were treated as described for NCYC132. The cdc7-GFP strain [S22] was incubated for live fluorescence imaging inside a CellAsic Y2 microfluidic chamber (CellAsic Corp., California, USA), with a constant flow of liquid YE at a rate of 5µl/h.

Microscopy of microcolony growth. Cells were imaged in a Zeiss Axiovert 200 microscope with a motorized XYZ stage. Metamorph (Molecular devices, California, USA) software was used to store 6 fixed positions on the stage corresponding to viewfields where one or two cells were visible. Bright-field images were acquired every minute for 21h (7-8 generations). Light exposure did not affect growth. Images were acquired with a Micromax NTE/CCD-1024-EB camera (Roper scientific, Tucson, USA), at 600x magnification (Plan-Neofluar 60x/1.40 Oil). Exposure time was 30ms (2.0V of 100W Halogen lamp). The maximal time resolution was 30 seconds.

Imaging cellular components labeled with GFP (spindle pole body and protein aggregates). The Cdc7-GFP protein co-localizes with the new spindle-pole body during anaphase, allowing the identification of the cell that inherits the New SPB (fluorescent signal) and the sister that inherits the Old SPB (no fluorescence signal). The Hsp104-GFP binds to protein aggregates and allows the estimation of the amount based on fluorescence intensity (a.u.). Both structures were followed ininterruptedly over several cell divisions. Cells were imaged in a DeltaVision core microscope, with a motorized XYZ stage (AppliedPrecision, USA). An Olympus UPlanSApo 100X 1.4NA Oil (R.I. 1.516) immersion objective was used (Olympus, Tokyo, Japan). The illumination was provided by a LED (transmitted light) and Lumicore solid-state illuminator (SSI-Lumencore, fluorescence), and the images were acquired with a Cool Snap HQ2 camera (Photometrics, Tucson, USA) and the SoftWorx software (AppliedPrecision, USA), using 2x2 pixel binning, to minimize light exposure (pixel size = 0.1288µm). For long-term time lapse imaging, Z-stacks for 6-12 non-overlapping imaging areas in the sample were acquired every 10 minutes (total time = 20h) and in short time-lapses every minute (total time = 1-3h). For single Z-stacks cells were imaged with exposure=0.05-0.20s, 2-50% transmission, depending on the protein and fluorescent label. As a control for photo-toxicity, cell cycle duration and protein aggregate number were measured and found similar in the presence and absence of continuous illumination.

Image analysis. The custom cell tracking software was developed using Microsoft Visual C++.NET. The initial cell in the microcolony is marked manually, and the tracking routine

marks the cell poles until the next division. Division of cells is marked by user input when septation occurs, and two new tracking routines mark the new daughter cells poles. The data of lineage and division time is automatically stored. We used division time instead of growth rate because we could determine the division time with high precision, while the growth rate is not well defined due to a complex growth pattern of *S. pombe* cells [S23]. After the cell tracking is completed, a custom java application was used to plot the information in pedigree trees. Division time is represented by the distance between the mother cell and its two siblings in the next generation, normalized by the average division time of the generation. Distinct pedigree lineages are represented by subsequent branches stemming from the cell that originated the microcolony. The mean division tree was designed by using the average of all the unique positions in a total of 52 trees (Figure 1A).

For analysis of cell length and symmetry of division (Figure S1F), the length was obtained by manually measuring the distance between cell poles (division length) and cell pole and division septum immediately before cell separation (birth length) using the ImageJ measure routine (NIH, Bethesda, USA). The pixel size was 200 nm.

Data analysis. Cell division times were normalized by the average division time of cells of the same generation in the same colony, in order to account for the changes in growth rate related to environmental changes and adaptation. The data is represented as mean ± standard error on the mean (SEM). For comparison of two samples, a two-tailed non-paired t-test was used at a confidence level of 95%.

Micromanipulation. The micromanipulation experiments were performed with a Singer MSM Manual Micromanipulator, equipped with a 20X LWD/0.30 long distance objective. Images were acquired with a 12-bit gray scale Sensicam camera (PCO, Kelheim, Germany) coupled to the micromanipulator. A custom written program running under Matlab (Mathworks) allowed acquiring and storing images at a fixed time interval. Spores of the strain NCYC132 were transferred with a microneedle to a yeast extract agar (YEA) plate sealed with parafilm to avoid drying. In the course of the experiment, siblings of cells inheriting the old pole or the new pole, respectively, were discarded from the viewfield, and images were acquired with an interval of 1 minute, during up to 4 days (T=23±2ºC). Division times were determined for the individual experiments.

Experiments with cells under stress conditions. Cells where protein aggregates were labelled with Hsp104-GFP that were growing vegetatively in liquid culture (YE) at 25ºC were subjected to two independent stress conditions: 40ºC water bath for 1h, and incubated in YE5 1mM H_2O_2 for 1h at 25ºC. A wide range of temperatures (36-42ºC) and H_2O_2 concentrations (0.1mM-10mM) were tested. Below 36ºC or 0.5mM H_2O_2 almost no arrest was observed, and above 42ºC or 2mM H_2O_2 most of the cells died without dividing. The arrest in growth before the first division (up to 10h), and the sudden increase in protein aggregation were used as the indicative of stress. Cells were grown initially at 25ºC for 7h in liquid media after the stress, then incubated in an agarose pad (YE5 without H_2O_2 following oxidative stress, and YE5 at T=37ºC following heat stress) as described above, for imaging. Then cells were monitored for 4-6 divisions.

Size exclusion chromatography and protein biochemistry. Cell lysates were obtained by concentrating 50-100 OD of cells from mid-exponential phase cultures (OD=0.6-1) in 500µl of lysis buffer (50mM Tris-HCl pH 7.5, 150mM NaCl, 5mM EDTA, 0.1% Triton X-100) with protease inhibitors (0.4mM PMSF, 8mM N-ethylmaleimide) and the cOmplete protease inhibitor cocktail (Roche Applied Science, Germany), and lysing the cells with glass beads (400µl of glass beads with a diameter between 0.25-0.50 mm, 25Hz, at 4°C for 20min). Cell debris and unlysed cells were pelleted by centrifugation at 1000G, 1min. Cell lysates were filtered in Spin-X columns (0.22µm pore size, cellulose acetate, Corning, USA) and 200µl of clear lysate was injected on a Superose 6 column (24ml, molecular weight range 10^4-10^7 Da, GE Healthcare Europe GmbH, Freiburg, Germany). Samples were eluted with 2xPBS. For detection upon transfer to a nitrocellulose membrane, rabbit polyclonal anti-Hsp104 R5 [S24] anti-actin (A2006, Sigma-Aldrich, Hannover, Germany), and mouse monoclonal anti-GAPDH (43700, Invitrogen, Darmstadt, Germany), anti-GFP (11814460001, Roche Applied Science, Germany) and anti-mCherry (700A10, MPI-CBG, Dresden, Germany) antibodies together with an HRP-conjugated antibody (Promega, USA) and Enhanced ChemiLuminescence detection (GE Healthcare Europe GmbH, Freiburg, Germany) were used.

Light scattering assay of cellular fractions. The UV absorption, together with the refraction index (R.I.) and light scattering of the fractions was measured using a UV detector (λ=240nm), light deflection of sample inside a 45° angle quartz glass and Right angle light scattering (90° angle, RALS) and Low Angle Light Scattering (7° angle, LALS) with a laser

diode as a light source (Malvern, England), respectively. The estimated molecular weight of the analyzed molecules for individual fractions was estimated from these measurements using the manufacturers software (Malvern, England).

Hsp104 expression and *in vitro* activity. Hsp104 from *S. pombe* was cloned in a pPROEX HTb (Invitrogen, Darmstadt, Germany) expression vector and purified from *E. coli* as described [S25] with modifications. The composition of the lysis buffer was altered to: 20mM Tris pH 8, 0.5mM EDTA, 5mM MgCl2, 2.5% glycerol (w/v), 50mM NaCl, cOmplete Mini EDTA-free protease inhibitor tabs (1tab/50ml) (Roche Applied Science, Germany), and 5μM pepstatin-A (Sigma-Aldrich). Cell lysates were clarified via centrifugation at 38,724g for 40min and the supernatant was directly applied to Q-Sepharose (GE Healthcare) followed by Resource Q anion exchange (GE Healthcare). The *in vitro* activity of Hsp104 from S. *pombe* was tested with a luciferase reactivation assay, where the luminescence recovery of urea-denatured luciferase aggregates was measured as described [S24]. Luciferase aggregates (50nM luciferase monomer) were incubated with either *S.cerevisiae* or *S. pombe* Hsp104 (1μM hexamer) for 90min at 25°C. To assess intrinsic Hsp104 disaggregase activity, reactions were supplemented with different ratios of ATPγS:ATP as indicated [S26]. Total nucleotide concentration was maintained at 5mM. To test whether Guanidine Hydrochloride (GuaHCl) inhibited the Hsp104 from *S. pombe* we measured the ATPase activity of *S. cerevisiae* and *S. pombe* Hsp104 (0.25μM) at 25°C in the presence of ATP (1mM) plus or minus GuaHCl (20mM). The amount of Pi (μM) released from ATP after 5min was determined using a Malachite Green based assay (Innova Biosciences, Cambridge, UK).

Quantification of aggregate number and amount. The number of aggregates in each cell was counted in a maximum intensity projection using Fiji, a freely distributed software. We assumed that puncta overlapping in z-stacks (same xy coordinates in consecutive z-slices) that moved coordinately correspond to a single aggregate. For Hsp104-GFP intensity quantification, the images were projected using the average intensity projection method (Fiji), which sums the intensity of pixels along the z-axis, at each time point. The area and total intensity of segmented puncta (Hsp104-GFP aggregates) was automatically measured using the "magic wand" function, using a fixed threshold.

SUPPLEMENTAL REFERENCES

S1. Winkler, J., Tyedmers, J., Bukau, B., and Mogk, A. (2012). Hsp70 targets Hsp100 chaperones to substrates for protein disaggregation and prion fragmentation. J Cell Biol *198*, 387-404.

S2. Nurse, P. (1975). Genetic control of cell size at cell division in yeast. Nature *256*, 547-551.

S3. Erjavec, N., Cvijovic, M., Klipp, E., and Nystrom, T. (2008). Selective benefits of damage partitioning in unicellular systems and its effects on aging. Proc Natl Acad Sci U S A *105*, 18764-18769.

S4. Aguilaniu, H., Gustafsson, L., Rigoulet, M., and Nystrom, T. (2003). Asymmetric inheritance of oxidatively damaged proteins during cytokinesis. Science *299*, 1751-1753.

S5. Minois, N., Frajnt, M., Dolling, M., Lagona, F., Schmid, M., Kuchenhoff, H., Gampe, J., and Vaupel, J.W. (2006). Symmetrically dividing cells of the fission yeast schizosaccharomyces pombe do age. Biogerontology *7*, 261-267.

S6. Barker, M.G., and Walmsley, R.M. (1999). Replicative ageing in the fission yeast Schizosaccharomyces pombe. Yeast *15*, 1511-1518.

S7. Calleja, G.B., Zuker, M., Johnson, B.F., and Yoo, B.Y. (1980). Analyses of fission scars as permanent records of cell division in Schizosaccharomyces pombe. J Theor Biol *84*, 523-544.

S8. Sahin, E., and Roberts, C.J. (2012). Size-Exclusion Chromatography with Multi-angle Light Scattering for Elucidating Protein Aggregation Mechanisms. Methods Mol Biol *899*, 403-423.

S9. Kaganovich, D., Kopito, R., and Frydman, J. (2008). Misfolded proteins partition between two distinct quality control compartments. Nature *454*, 1088-1095.

S10. Parsell, D.A., Kowal, A.S., Singer, M.A., and Lindquist, S. (1994). Protein disaggregation mediated by heat-shock protein Hsp104. Nature *372*, 475-478.

S11. Senechal, P., Arseneault, G., Leroux, A., Lindquist, S., and Rokeach, L.A. (2009). The Schizosaccharomyces pombe Hsp104 disaggregase is unable to propagate the [PSI] prion. PLoS One *4*, e6939.

S12. Winter, J., Ilbert, M., Graf, P.C., Ozcelik, D., and Jakob, U. (2008). Bleach activates a redox-regulated chaperone by oxidative protein unfolding. Cell *135*, 691-701.

S13. Gragerov, A.I., Martin, E.S., Krupenko, M.A., Kashlev, M.V., and Nikiforov, V.G. (1991). Protein aggregation and inclusion body formation in Escherichia coli rpoH mutant defective in heat shock protein induction. FEBS Lett *291*, 222-224.

S14. Narayanaswamy, R., Levy, M., Tsechansky, M., Stovall, G.M., O'Connell, J.D., Mirrielees, J., Ellington, A.D., and Marcotte, E.M. (2009). Widespread reorganization of metabolic enzymes into reversible assemblies upon nutrient starvation. Proc Natl Acad Sci U S A *106*, 10147-10152.

S15. Noree, C., Sato, B.K., Broyer, R.M., and Wilhelm, J.E. (2010). Identification of novel filament-forming proteins in Saccharomyces cerevisiae and Drosophila melanogaster. J Cell Biol *190*, 541-551.

S16. Grimminger, V., Richter, K., Imhof, A., Buchner, J., and Walter, S. (2004). The prion curing agent guanidinium chloride specifically inhibits ATP hydrolysis by Hsp104. J Biol Chem *279*, 7378-7383.

S17. Landgraf, D., Okumus, B., Chien, P., Baker, T.A., and Paulsson, J. (2012). Segregation of molecules at cell division reveals native protein localization. Nat Methods *9*, 480-482.

S18. Roux, A.E., Leroux, A., Alaamery, M.A., Hoffman, C.S., Chartrand, P., Ferbeyre, G., and Rokeach, L.A. (2009). Pro-aging effects of glucose signaling through a G protein-coupled glucose receptor in fission yeast. PLoS Genet *5*, e1000408.
S19. Miyata, M., Miyata, H., and Johnson, B.F. (2000). Sibling differences in cell death of the fission yeast, Schizosaccharomyces pombe, exposed to stress conditions. Antonie Van Leeuwenhoek *78*, 203-207.
S20. Forsburg, S.L., and Rhind, N. (2006). Basic methods for fission yeast. Yeast *23*, 173-183.
S21. Bahler, J., Wu, J.Q., Longtine, M.S., Shah, N.G., McKenzie, A., 3rd, Steever, A.B., Wach, A., Philippsen, P., and Pringle, J.R. (1998). Heterologous modules for efficient and versatile PCR-based gene targeting in Schizosaccharomyces pombe. Yeast *14*, 943-951.
S22. Sohrmann, M., Schmidt, S., Hagan, I., and Simanis, V. (1998). Asymmetric segregation on spindle poles of the Schizosaccharomyces pombe septum-inducing protein kinase Cdc7p. Genes Dev *12*, 84-94.
S23. Baumgartner, S., and Tolic-Norrelykke, I.M. (2009). Growth pattern of single fission yeast cells is bilinear and depends on temperature and DNA synthesis. Biophys J *96*, 4336-4347.
S24. Glover, J.R., and Lindquist, S. (1998). Hsp104, Hsp70, and Hsp40: a novel chaperone system that rescues previously aggregated proteins. Cell *94*, 73-82.
S25. Sweeny, E.A., DeSantis, M.E., and Shorter, J. (2011). Purification of hsp104, a protein disaggregase. J Vis Exp.
S26. Doyle, S.M., Shorter, J., Zolkiewski, M., Hoskins, J.R., Lindquist, S., and Wickner, S. (2007). Asymmetric deceleration of ClpB or Hsp104 ATPase activity unleashes protein-remodeling activity. Nat Struct Mol Biol *14*, 114-122.